

Inverse Synthetic Aperture Radar Imaging Based on the Non-Convex Regularization Model

Yanan ZHAO¹, Fengyuan YANG¹, Chao WANG¹, Fangjie YE², Feng ZHU¹, Yu LIU¹

¹ The Nanjing Research Institute of Electronic Engineering, Nanjing 210007, China

² School of Mathematical Sciences, Nankai University, Tianjin 300110, China

mathzyn@mail.nankai.edu.cn, 653497400@qq.com, {diguatongxue, yfj160032, liuyu_2002}@163.com, fenix_zh@126.com

Submitted July 27, 2023 / Accepted November 29, 2023 / Online first December 18, 2023

Abstract. *Compressed Sensing (CS) has been shown to be an effective technique for improving the resolution of inverse synthetic aperture radar (ISAR) imaging and reducing the hardware requirements of radar systems. In this paper, our focus is on the ℓ_p ($0 < p < 1$) model, which is a well-known non-convex and non-Lipschitz regularization model in the field of compressed sensing. In this study, we propose a novel algorithm, namely the Accelerated Iterative Support Shrinking with Full Linearization (AISSFL) algorithm, which aims to solve the ℓ_p regularization model for ISAR imaging. The AISSFL algorithm draws inspiration from the Majorization-Minimization (MM) iteration algorithm and integrates the principles of support shrinkage and Nesterov's acceleration technique. The algorithm employed in this study demonstrates simplicity and efficiency. Numerical experiments demonstrate that AISSFL performs well in the field of ISAR imaging.*

Keywords

ISAR, compressed sensing, non-convex optimization, AISSFL algorithm

1. Introduction

Inverse Synthetic Aperture Radar (ISAR) has gained significant popularity in both military and civilian domains owing to its capability to generate images of non-cooperative maneuvering targets [1–4]. In order to acquire a high-resolution image, it is imperative to transmit signals with a wide bandwidth and extend the duration of coherent accumulation. However, this will result in an escalation in the complexity associated with the collection, transmission, and storage of data. Consequently, this will impose a significant strain on the radar hardware. Compressed sensing has shown that when a signal is sparse, it can be reconstructed using a sampling rate significantly lower than what is required by Shannon's sampling theorem [5–7]. Fortunately, the ISAR image exhibits sparsity in the Doppler domain,

thereby enabling the utilization of compressed sensing techniques to improve resolution and minimize the data demands for ISAR imaging [8–10].

Radar image reconstruction based on compressed sensing theory is a classic inverse problem, which is to reconstruct the original radar signal on the basis of the known observed signal and the known observation matrix. Assumed that the translational motion of the target has been fully compensated using conventional methods. Considering the impact of noise, the observation process can be formulated as [11], [12]

$$\mathbf{y} = \Phi \mathbf{x} + \mathbf{b} \quad (1)$$

where $\mathbf{y} \in \mathbb{C}^m$ is the observed signal, $\mathbf{b} \in \mathbb{C}^n$ is the noise in the observation, $\Phi \in \mathbb{C}^{m \times n}$ ($m < n$) is the observation matrix which is used to observe the high-dimensional original signal \mathbf{x} and obtain the low-dimensional observed value \mathbf{y} , and $\mathbf{x} \in \mathbb{C}^n$ is the radar signal to be reconstructed. Since the equation presented in (1) is an underdetermined system, it possesses an infinite number of solutions. Consequently, it is not possible to reconstruct the original signal solely based on this system.

Compressed sensing asserts that if the radar signal \mathbf{x} exhibits sparsity under an orthogonal basis or tight frame Ψ , i.e., $\mathbf{x} = \Psi \alpha$, and the given equation (1) can be expressed as

$$\mathbf{y} = \Phi \Psi \alpha + \mathbf{b} \quad (2)$$

where $\alpha \in \mathbb{C}^n$ is the sparse representation of \mathbf{x} under Ψ , and Ψ is irrelevant to Φ . Then, the approximate value $\tilde{\alpha}$ of α can be obtained by solving a nonlinear optimization problem based on the known observed signal \mathbf{y} and observation matrix Φ and noise type. Moreover, the original signal \mathbf{x} is restored by $\mathbf{x} = \Psi \tilde{\alpha}$. Let $\Phi \Psi = \Theta$, where $\Theta \in \mathbb{C}^{m \times n}$ ($m < n$) is referred to as the sensing matrix. The product of the observation matrix Φ and the sparse basis matrix Ψ must satisfy the Restricted Isometry Property (RIP) condition [6], [7] to ensure accurate reconstruction of the signal.

When designing a measurement matrix Φ , the key factors are the measurement waveform and sampling method. Commonly used observation matrices can be mainly divided

into three categories. The first category consists of completely random observation matrices, such as Gaussian random observation matrices and Bernoulli random observation matrices. The elements of this type of matrix follow independent distributions and remain incoherent with general orthogonal bases. The reconstructed signal has high accuracy and is the most common and applicable measurement matrix. However, it is difficult to implement in hardware; The second type is structural random observation matrices, such as partial Fourier matrices, partial Hadamard matrices and non-correlated measurement matrices, etc., which are obtained by randomly extracting some rows from an orthogonal matrix and then normalizing them. This type of matrix is easy to implement and store, and has high reconstruction accuracy; The third category is deterministic observation matrices, such as Toeplitz matrices, circulant matrices, etc. These matrices are proposed for specific signals. This type of matrix is easy to implement in hardware and design fast algorithms, but the reconstruction accuracy is low.

The compressed sensing model presented in (2) is still an underdetermined system. However, by incorporating the sparse prior information of α to constrain the solution space, it becomes feasible to reconstruct the original radar signal. This is due to the fact that the most sparse solution has the potential to be the accurate solution. For this model, there exist some solution methods. Two commonly employed solution methods are greedy methods and regularization methods. The Orthogonal Matching Pursuit (OMP) algorithm, as described in reference [13], is a well-known greedy algorithm commonly used in ISAR imaging. The algorithm exhibits several advantages, including simplicity, efficiency, and ease of comprehension. However, it is important to note that a notable disadvantage of this algorithm is its susceptibility to noise interference. Regularization algorithms can be broadly categorized into two types: convex regularization algorithms and non-convex regularization algorithms. Based on the sparsity of signals, the ℓ_0 "norm" is utilized as the regularization term. The ℓ_0 regularization model is

$$\min_{\alpha \in \mathbb{C}^n} \lambda \|\alpha\|_0 + \frac{1}{2} \|\Theta\alpha - \mathbf{y}\|_2^2 \quad (3)$$

where $\lambda > 0$ serves as the regularization parameter, and the notation $\|\alpha\|_0$ denotes the cardinality of the set $\{i : \alpha_i \neq 0\}$, which counts the number of non-zero elements in the vector α . In this context, the $\|\alpha\|_0$ "norm" represents the regularized term, and the term $\frac{1}{2} \|\Theta\alpha - \mathbf{y}\|_2^2$ corresponds to the data fitting term. Theoretically, it is possible to obtain the optimal solution of the ℓ_0 regularization. However, it should be noted that this problem is classified as NP-hard [14]. As a result, solving it directly in large-scale problems is not considered practical.

One approach to address the ℓ_0 regularization problem is through the use of convex relaxation, wherein the ℓ_1 norm is employed as a substitute for the ℓ_0 "norm". The ℓ_1 regularization model [15] is

$$\min_{\alpha \in \mathbb{C}^n} \lambda \|\alpha\|_1 + \frac{1}{2} \|\Theta\alpha - \mathbf{y}\|_2^2 \quad (4)$$

where $\|\alpha\|_1 = \sum_{i=1}^n |\alpha_i|$. The problem in equation (4) pertains to the classical Basis Pursuit (BP) problem, as discussed in reference [16]. The ℓ_1 regularization is a convex optimization problem that has the ability to produce sparse solutions [17]. E. Candès and Tao has proved that under the Restricted Isometry Property (RIP) condition, the ℓ_1 regularization model and the ℓ_0 regularization model have the same solution [18]. There are some simple and efficient algorithms that have been developed for the ℓ_1 regularization model in the ISAR imaging problem. For instance, in references [19], [20], a smooth function is formulated as a substitute for the ℓ_1 term, and the solution is obtained through the application of the derivative operation. Additionally, in another studies [21], [22], the Alternating Direction Method of Multipliers (ADMM) algorithm is employed to solve the ℓ_1 regularization model for ISAR imaging. In [23], the Iterative Soft Thresholding (IST) algorithm is utilized to solve the ℓ_1 regularization model, among other methods.

In recent years, there has been an increasing body of research indicating that the accuracy of the solution to the ℓ_1 regularization model is not satisfactory and the sparsity of the reconstructed signal often deviates from the expected level. Conversely, it has been observed that the non-convex regularization model outperforms the convex regularization model, as supported by several studies [24–27]. For instance, in the study conducted by the authors [24], it was noted that the non-convex regularization model has the ability to utilize a smaller amount of measurement data compared to the convex regularization model for signal reconstruction. Additionally, the non-convex regularization model demonstrates higher accuracy in the reconstruction process. In this paper, we consider the classical non-convex ℓ_p ($0 < p < 1$) regularization model:

$$\min_{\alpha \in \mathbb{C}^n} \lambda \|\alpha\|_p + \frac{1}{2} \|\Theta\alpha - \mathbf{y}\|_2^2 \quad (5)$$

where $\|\alpha\|_p = \sum_{i=1}^n |\alpha_i|^p$. The optimization problem stated in (5) is characterized as non-convex and non-Lipschitz, thereby posing a significant challenge in devising an algorithm for this particular model. There are already many algorithms for solving the ℓ_p ($0 < p < 1$) regularization model in ISAR imaging, such as researchers specifically focused on the $\ell_{1/2}$ regularization model and designed an algorithm for this model [28], [29]. In the study referenced as [30], the iterative weighted ℓ_1 method (IRL1) was utilized to solve the ℓ_p model. Additionally, in another study referenced as [11], the block iterative reweighted ℓ_2/ℓ_p minimization algorithm (BIRL2- ℓ_p) was proposed for ISAR imaging, among others.

In this paper, we present a novel algorithm called the AISSFL algorithm, which aims to address the ℓ_p regularization problem in ISAR imaging. The AISSFL algorithm draws inspiration from the Majorization-Minimization (MM) iteration algorithm and incorporates the concepts of support shrinkage and Nesterov's acceleration technique. The MM iterative algorithm [31] is not only a specific algorithm, but also a framework for algorithms. The MM algorithm solves

optimization problems iteratively by minimizing a surrogate majorizing function of the objective function at each iteration. For the ℓ_p regularization model, the surrogate function is constructed by utilizing the first-order Taylor expansion of the regularization term and the second-order Taylor expansion of the data fitting term. The surrogate function that we construct is a strongly convex function, thereby ensuring the existence of a unique analytical solution at each iteration. The strategy of support set shrinkage [32], could overcome the non-Lipschitz of the objective function at the zero, and avoid the weight value in the surrogate function becoming infinite. The algorithm we have developed falls under the category of gradient methods, thus making it suitable for the application of Nesterov's acceleration technique [33] to enhance its performance. The AISSFL algorithm possesses an analytical solution at each iteration, thereby making it a single-loop algorithm characterized by high efficiency. In Sec. 2, a comprehensive explanation of this algorithm is provided. In Sec. 3, the numerical experiments demonstrate that the AISSFL algorithm exhibits excellent performance in ISAR imaging, surpassing several renowned algorithms.

2. Algorithm

In this section, we give the design process of the AISSFL algorithm. AISSFL is a process of reconstructing the radar signal \mathbf{x} based on the existing observation \mathbf{y} and known the sensing matrix Θ .

Firstly, it should be noted that the function $h(x) = x^p$ ($0 < p < 1$) is non-Lipschitz at zero. Consequently, the objective function in (4) is a non-convex and non-Lipschitz function. Non-Lipschitz properties will result in the weight value, as described later, becoming infinite. Therefore, in the algorithm, if certain optimization variables are determined to be zero in the k -th step, we consistently assign these variables a value of zero and exclude them from further calculations in subsequent iterations. In general, the support set of a vector $\alpha \in \mathbb{C}^n$ is defined as $\Omega(\alpha) := \{i \in [n] : |\alpha_i| \neq 0\}$, where $[n] = \{1, 2, \dots, n\}$. Considering the limited word length of actual computers and in order to prevent excessively large linearization weights as described subsequently, the support set of a vector $\alpha \in \mathbb{C}^n$, we define its support set as

$$\Omega(\alpha) := \{i \in [n] : |\alpha_i| \geq \varepsilon\} \quad (6)$$

where ε represents a small positive number, and we use the notation $\Omega(\alpha^k)$ as an abbreviation for Ω^k . That is to say, in the algorithm, if a variable is smaller than a specified precision, it is also considered as zero. Based on the support set shrinkage strategy, the unconstrained ℓ_p regularization problem stated in (5) can be reformulated as into a constrained optimization problem. The value of α^{k+1} is determined by solving the following constrained optimization problem

$$\begin{aligned} \alpha^{k+1} = \arg \min_{\alpha \in \mathbb{C}^n} & \left\{ \lambda \|\alpha\|_p + \frac{1}{2} \|\Theta\alpha - \mathbf{y}\|_2^2 \right\} \\ \text{s.t. } & \alpha_i^{k+1} = 0, \forall i \in [n] \setminus \Omega^k. \end{aligned} \quad (7)$$

The support shrinkage strategy can not only overcome the non-Lipschitz property of the objective function but also reduce the scale of the problem to be solved in each iteration.

Next, the problem stated in (7) remains a non-convex optimization problem. Inspired by the MM algorithm, we employ the Taylor expansion technique to approximate the objective function as a surrogate function at each iteration. In this approach, the regularization term is approximated using a first-order Taylor expansion, while the data fitting term is approximated using a second-order Taylor expansion. In every iteration, the surrogate function is minimized. The value of α^{k+1} is determined by solving the following problem:

$$\begin{aligned} \min_{\alpha \in \mathbb{C}^n} & \left\{ \lambda \sum_{i \in \Omega^k} \left[|\alpha_i^k|^p + p|\alpha_i^k|^{p-1}(|\alpha_i| - |\alpha_i^k|) \right] + \frac{1}{2} \|\Theta\alpha^k - \mathbf{y}\|_2^2 \right\} \\ & + (\alpha - \alpha^k)^T \Theta^T (\Theta\alpha^k - \mathbf{y}) + \frac{\gamma}{2} \|\alpha - \alpha^k\|_2^2 \\ \text{s.t. } & \alpha_i^{k+1} = 0, \forall i \in [n] \setminus \Omega^k \end{aligned} \quad (8)$$

where $\gamma \geq \|\Theta^T \Theta\|_2$. The problem in (8) is a strongly convex optimization problem, thus it is easy to solve.

Nesterov's acceleration method [33] is a highly efficient technique for acceleration. We have observed that the utilization of Nesterov's acceleration technique yields a significant acceleration effect for gradient algorithms. The algorithm described in (8) is classified as a gradient algorithm. To enhance its performance, we employ Nesterov's acceleration technique. Herein, we introduce a new variable β^k defined as

$$\beta^k = \alpha^k + t_k(\alpha^k - \alpha^{k-1}) \quad (9)$$

where

$$t_k = \frac{c_{k-1} - 1}{c_k}, \quad c_{k+1} = \frac{1 + \sqrt{1 + 4c_k^2}}{2}, \quad c_{-1} = c_0 = 1, \quad (10)$$

is the parameter of extrapolation. After acceleration, the α^{k+1} is obtained by solving the following problem:

$$\begin{aligned} \min_{\alpha \in \mathbb{C}^n} & \left\{ \lambda \sum_{i \in \Omega^k} \left[|\alpha_i^k|^p + p|\alpha_i^k|^{p-1}(|\alpha_i| - |\alpha_i^k|) \right] + \frac{1}{2} \|\Theta\beta^k - \mathbf{y}\|_2^2 \right\} \\ & + (\alpha - \beta^k)^T \Theta^T (\Theta\beta^k - \mathbf{y}) + \frac{\gamma}{2} \|\alpha - \beta^k\|_2^2 \\ \text{s.t. } & \alpha_i^{k+1} = 0, \forall i \in [n] \setminus \Omega^k. \end{aligned} \quad (11)$$

Now, we solve the problem in (11). By combining similar terms, we get

$$\begin{aligned} & \frac{1}{2} \|\Theta\beta^k - \mathbf{y}\|_2^2 + (\alpha - \beta^k)^T \Theta^T (\Theta\beta^k - \mathbf{y}) \\ & + \frac{\gamma}{2} \|\alpha - \beta^k\|_2^2 = \frac{\gamma}{2} \|\alpha - \eta^k\|_2^2 + C \end{aligned} \quad (12)$$

where $\eta^k = \beta^k - \frac{1}{\gamma} \Theta^T (\Theta\beta^k - \mathbf{y})$ and C is a constant. Therefore, the objective function in (11) is separable for each indicator i . Then, the problem stated in (11) can be equivalently expressed as

$$\begin{cases} \alpha_i^{k+1} = \arg \min_{\alpha} \sum_{i \in \Omega^k} [w_i^k |\alpha_i| + \frac{\gamma}{2} (\alpha_i - \eta_i^k)^2], \forall i \in \Omega^k; \\ \alpha_i^{k+1} = 0, & \forall i \in [n] \setminus \Omega^k \end{cases} \quad (13)$$

where $w_i^k = \lambda p |\alpha_i^k|^{p-1}$. The problem in (13) has the following analytic solution [34]:

$$\alpha_i^{k+1} = \max \left\{ 0, 1 - \frac{w_i^k}{\gamma |\eta_i^k|} \right\} \eta_i^k, \forall i \in \Omega^k. \quad (14)$$

In summary, we give the AISSFL algorithm in Algorithm 1.

Algorithm 1. The Accelerated Iterative Support Shrinking with Full Linearization algorithm (AISSFL).

Input: The observation \mathbf{y} and the sensing matrix Θ .

Set parameter: $\lambda, \gamma, \varepsilon, \alpha^0, k := 1, \varepsilon, \text{Maxit}$.

1. Find support set: $\Omega^k = \{i \in [n] : |\alpha_i^k| \geq \varepsilon\}$.

2. Update weight: $w_i^k = \lambda p |\alpha_i^k|^{p-1}$.

3. Compute α^{k+1} :

$$\begin{cases} \alpha_i^{k+1} = \max \left\{ 0, 1 - \frac{w_i^k}{\gamma |\eta_i^k|} \right\} \eta_i^k, \forall i \in \Omega^k; \\ \alpha_i^{k+1} = 0, & \forall i \in [n] \setminus \Omega^k. \end{cases} \quad (15)$$

4. If the relative error $\frac{\|\alpha^{k+1} - \alpha^k\|_2}{\|\alpha^k\|_2} > \varepsilon$ or $k < \text{Maxit}$, let $k = k + 1$ and return to step 1, step 2, step 3.

Output α^{k+1} .

The reconstructed radar signal $\mathbf{x} = \Psi \alpha$, and the ISAR image can be obtained by applying the Fast Fourier Transform (FFT) to \mathbf{x} . The AISSFL algorithm is a single-loop algorithm, which is easy to implement and efficient. The numerical experiments in Sec. 3 show that the AISSFL algorithm performs well.

3. Numerical Experiments

In this section, the AISSFL algorithm is employed for the purpose of 2D inverse synthetic aperture radar imaging. Subsequently, a comparison is made between the AISSFL algorithm, the OMP algorithm, the IST algorithm and $\ell_{\frac{1}{2}}$ algorithm. All experiments were completed on a desktop computer with Windows 7, 64bit, 8 GB memory, Intel Core™ i7-7700 CPU (3.60 GHz). MATLAB R2016a is mathematical software. The simulation data is the 64×512 dimensional MIG-25 fighter echo data provided by V.C.CHEN of the US Air Force Laboratory. The radar carrier frequency is 9 GHz, the bandwidth is 512 MHz, and the pulse repetition frequency is 15 kHz. The echo data has completed motion compensation and can be directly imaged.

3.1 Experimental Setup

In the experiment, a 64×128 data segment is chosen from the MIG-25 fighter echo data as the simulation signal, denoted as $\mathbf{x} = (x_1, \dots, x_{64})$, where $x_i \in \mathbb{C}^{128}$. This data segment is transformed using the Fast Fourier Transform (FFT) and is depicted in Fig. 1(a).

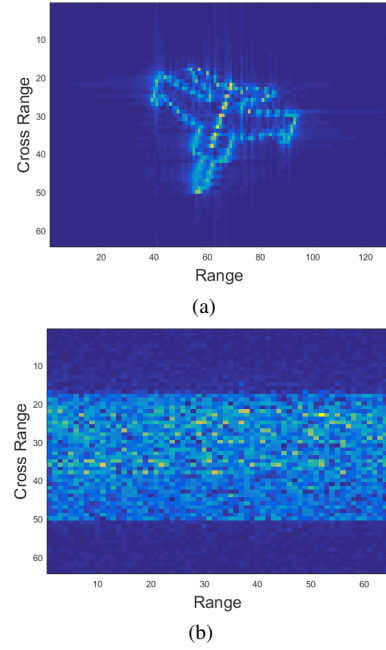


Fig. 1. The simulation signal and the observation signal.

The simulation data does not contain noise. To assess the performance of the AISSFL algorithm in the presence of noise, we introduce white Gaussian noise to the simulation data, so that the signal-to-noise ratio of the superimposed signal is 10 dB. The observation signal, denoted as $\mathbf{y} = (y_1, \dots, y_{64})$ where $y_i \in \mathbb{C}^{64}$, is simulated according to the following procedure:

$$y_i = \Phi x_i + b \quad \forall i \in \{1, \dots, 64\} \quad (16)$$

where $\Phi \in \mathbb{C}^{64 \times 128}$ is the sensing matrix, b is the white Gaussian noise. The variable \mathbf{y} is depicted in Fig. 1(b). It is evident that the number of columns in matrix \mathbf{y} is half that of matrix \mathbf{x} . Collecting the compressed observation signal and subsequently reconstructing the original signal from the observation signal, rather than directly collecting the original signal, can significantly alleviate the hardware demands of radar systems, which is the significance of compressed sensing technology.

It is well-established that the radar echo signal exhibits sparsity in the Doppler domain. Therefore, we opt to utilize the orthogonal Fourier basis, denoted as $\Psi \in \mathbb{C}^{128 \times 128}$, as the sparse basis. Additionally, we select the observation matrix Φ to be a random Gaussian matrix. The sensing matrix $\Theta = \Phi \Psi$ constructed in this manner satisfies the Restricted Isometry Property (RIP) condition. In the proposed AISSFL, the parameter values are selected as follows: $\lambda = 2 \times 10^5$, $\gamma = \|\Theta^T \Theta\|_2^2$, $\varepsilon = 10^{-6}$, $\epsilon = 10^{-5}$, $\text{Maxit} = 100$, $p = 0.5$. The entropy value is utilized to assess the fidelity of the reconstructed image. The relationship between entropy and image aggregation is such that as entropy decreases, the degree of image aggregation increases, resulting in a higher quality of the reconstructed image. Conversely, as the entropy increases, the image becomes more chaotic, resulting

in a decrease in the quality of the reconstructed image. In experimental settings, the MATLAB software's "entropy" function is employed to compute the entropy of two-dimensional reconstructed images.

3.2 ISAR Imaging

The AISSFL algorithm is employed to address the ℓ_p regularization problem (5), resulting in an optimal solution denoted as $\bar{\alpha}$. Subsequently, the reconstructed radar signal is obtained as $\bar{\mathbf{x}} = \Psi\bar{\alpha}$. The ISAR image is reconstructed using the Fast Fourier Transform for $\bar{\mathbf{x}}$.

The ISAR image is depicted in Fig. 2(a). It is evident from Fig. 2(a) that the ISAR image reconstructed by AISSFL is of high quality, without the influence of side lobes and bad points. We chose a different data segment and applied the identical algorithm parameters to reconstruct it. The outcome

is depicted in Fig. 2(b). It is evident from Fig. 2(b) that the AISSFL algorithm is capable of reconstructing high-quality ISAR images from various perspectives in these parameters.

3.3 Adaptability to Different Type of Φ

In this subsection, we have chosen four other observation matrices that are frequently utilized to evaluate the effectiveness of the AISSFL algorithm. These matrices include the random Bernoulli matrix, the random PartHadamard matrix, the random PartFourier matrix, and the random Circulant matrix. The ISAR imaging results obtained using various observation matrices are depicted in Fig. 3. It is evident from Fig. 3 that the AISSFL algorithm demonstrates strong performance, with the exception of a few outliers in the reconstructed image when using the random cyclic matrix. This observation highlights the broad applicability of the AISSFL algorithm.

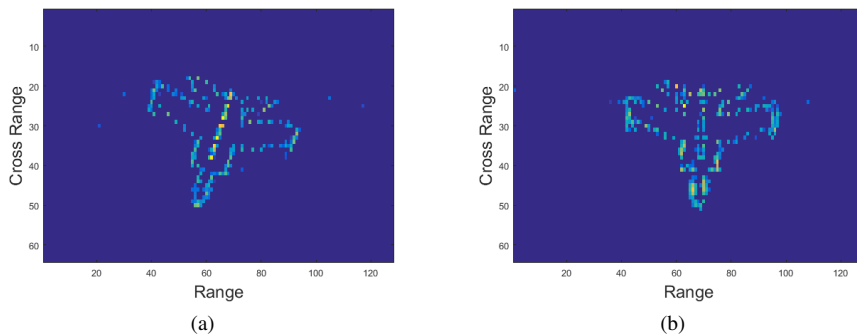


Fig. 2. The ISAR image reconstructed by the AISSFL algorithm.

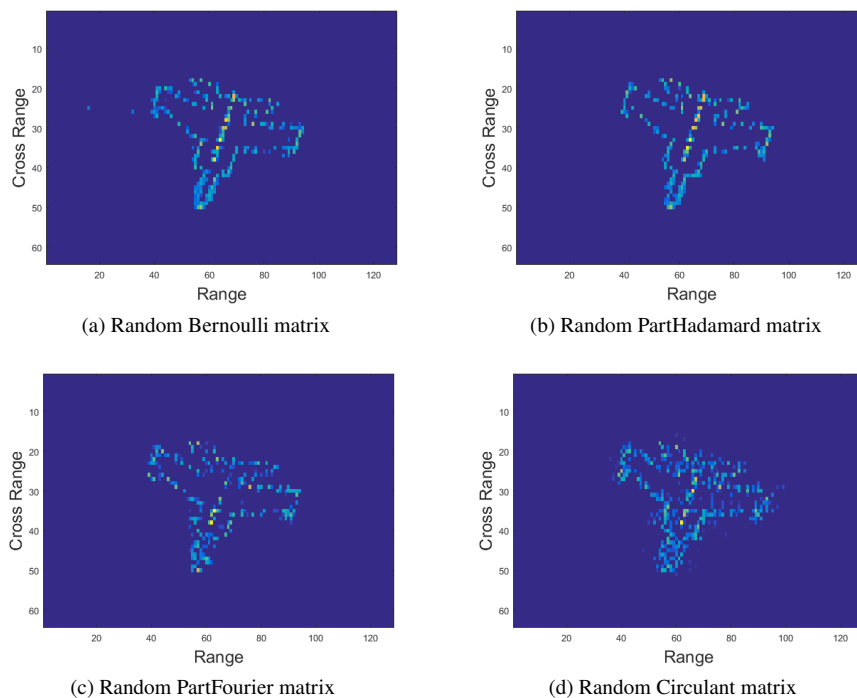


Fig. 3. The ISAR image is reconstructed using the AISSFL algorithm with various types of observation matrices.

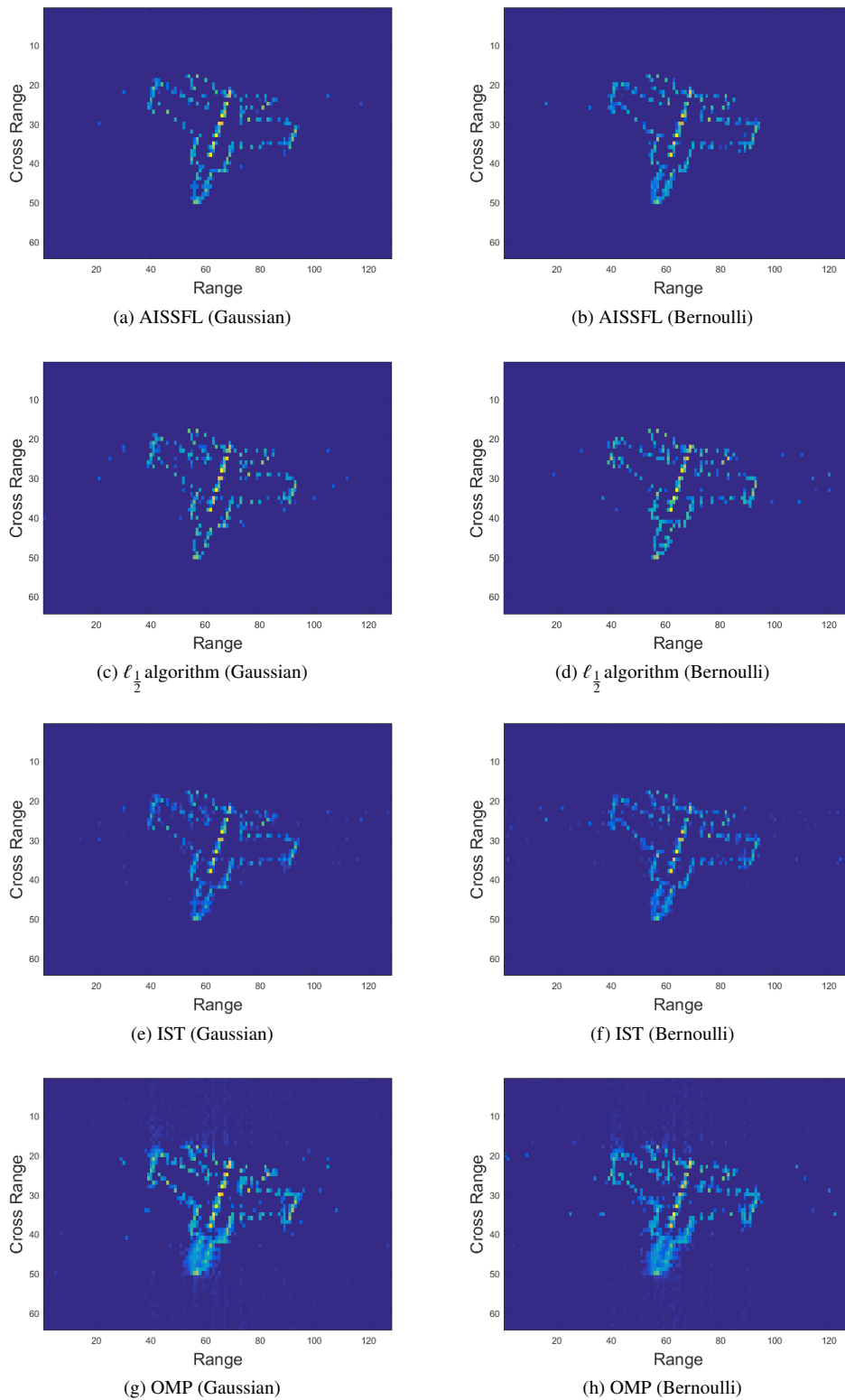


Fig. 4. The reconstructed images using the AISSFL algorithm, the ℓ_1 algorithm, the IST algorithm, and the OMP algorithm in ISAR imaging. The matrices shown in (a), (c), (e), (g) represent random Gaussian matrices, while the matrices in (b), (d), (f), (h) represent random Bernoulli matrices.

3.4 Adaptability to Different p

In this subsection, we examine the impact of the parameter p on the AISSFL algorithm. We consider the values of p to be 0.1, 0.3, 0.5, 0.7, and 0.9. The results of the entropy analysis are presented in Tab. 1. It is evident from the data presented in Tab. 1 that the entropies of the reconstructed images exhibit minimal variation across different values of p . This observation suggests that the AISSFL algorithm demonstrates robustness with respect to the parameter p .

3.5 Comparisons to Some Well-Known Algorithms

In this section, a comparison is made between the AISSFL algorithm and some well-known compressed sensing algorithms, namely the OMP algorithm [12], the IST algorithm [23] and $\ell_{\frac{1}{2}}$ algorithm [28]. We conducted experiments using two different types of observation matrices: the random Gaussian matrix and the random Bernoulli matrix. The reconstructed images obtained from Inverse Synthetic Aperture Radar (ISAR) are depicted in Fig. 4. The entropy of the reconstructed ISAR image and the CPU time (in seconds) are presented in Tab. 2.

It is evident from the comparison shown in Fig. 4 and the entropy value presented in the Tab. 2 demonstrate that the ISAR image reconstructed using the AISSFL algorithm exhibits superior clarity, with minimal artifacts. Additionally, the entropy value associated with the AISSFL algorithm is similar to the $\ell_{\frac{1}{2}}$ algorithm, and lower than the IST algorithm and the OMP algorithm. In relation to CPU time, the AISSFL algorithm demonstrates a similar performance to the IST algorithm. In addition, the $\ell_{\frac{1}{2}}$ algorithm takes the most time and the OMP algorithm takes the least time. Experiments have demonstrated that the AISSFL algorithm is a simple and effective method, exhibiting excellent performance in addressing the ISAR imaging problem. Previous studies frequently employ the terms "complex" and "sensitive to parameters" to characterize non-convex algorithms. However, the AISSFL algorithm is a simple and efficient algorithm, and it has only one regularization parameter λ to debug, the algorithm performs well when the parameter λ is between 60000 and 200000, which breaks the previous impression that non-convex algorithms are complex and sensitive to parameters.

| p | 0.1 | 0.3 | 0.5 | 0.7 | 0.9 |
|---------|------|------|------|------|-----|
| Entropy | 0.16 | 0.17 | 0.17 | 0.18 | 0.2 |

Tab. 1. The value of entropy of ISAR images reconstructed by AISSFL with different values of p .

| | AISSFL | $\ell_{\frac{1}{2}}$ algorithm | IST | OMP |
|-----------|--------------|--------------------------------|--------------|--------------|
| Gauss | 0.17, 0.51 s | 0.17, 1.04 s | 0.28, 0.39 s | 0.47, 0.25 s |
| Bernoulli | 0.19, 0.50 s | 0.20, 1.10 s | 0.29, 0.44 s | 0.47, 0.12 s |

Tab. 2. The value of entropy and CPU time (s) of the AISSFL algorithm, $\ell_{\frac{1}{2}}$ algorithm, the IST algorithm, and the OMP algorithm.

4. Conclusion

In this paper, we present a novel algorithm called AISSFL, which aims to solve the non-convex ℓ_p regularization model. AISSFL is a simple and efficient algorithm, breaking the conventional belief that non-convex algorithms are inherently complex and highly sensitive to parameter settings. We employ the AISSFL algorithm for the purpose of inverse synthetic aperture radar (ISAR) imaging. Numerical experiments demonstrate that the AISSFL algorithm exhibits strong performance across various values of $p \in (0, 1)$ and different observation matrices. Comparative experiments demonstrate that the ISAR image reconstructed using the AISSFL algorithm exhibits superior clarity compared to the $\ell_{\frac{1}{2}}$ algorithm, the IST algorithm and the OMP algorithm.

References

- [1] HAJDUCH, G., GARELLO, R., LE CAILLEC, J.-M., et al. High resolution snapshot SAR/ISAR imaging of ship targets at sea. *Proceedings of SPIE - SAR Image Analysis, Modeling, and Techniques V*, 2002, vol. 4883, p. 39–47. DOI: 10.1117/12.461899
- [2] LAZAROV, A. D., MINCHEV, C. N. ISAR Image reconstruction and autofocusing procedure over phase modulated signals. In *International Radar Conference*. Edinburgh (UK), 2002, p. 536–541. DOI: 10.1049/cp:20020344
- [3] PRICKET, M. J., CHEN, C. C. Principle of inverse synthetic aperture radar (ISAR) imaging. In *Electronics and Aerospace Systems Conference (EASCON)*. Arlington (USA), 1980, p. 340–345. ISSN: 0531-6863
- [4] WEHNER, D. R. *High-Resolution Radar*. Norwood: Artech House, 1987. ISBN: 0890061947
- [5] DONOHO, D. L. Compressed sensing. *IEEE Transactions on Information Theory*, 2006, vol. 52, no. 4, p. 1289–1306. DOI: 10.1109/TIT.2006.871582
- [6] CANDÉS, E. J., ROMBERG, J. K., TAO, T. Robust uncertainty principles: Exact signal reconstruction from highly incomplete frequency information. *IEEE Transactions on Information Theory*, 2006, vol. 52, no. 2, p. 489–509. DOI: 10.1109/TIT.2005.862083
- [7] CANDÉS, E. J., ROMBERG, J. K., TAO, T. Stable signal recovery from incomplete and inaccurate measurements. *Communications on Pure and Applied Mathematics*, 2006, vol. 59, no. 8, p. 1207–1223. DOI: 10.1002/cpa.20124
- [8] BARANIUK, R., STEEGHS, P. Compressive radar imaging. In *IEEE Radar Conference*. Waltham (USA), 2007, p. 128–133. DOI: 10.1109/RADAR.2007.374203
- [9] POTTER, L. C., PARKER, J. T. Sparsity and compressed sensing in radar imaging. *Proceedings of the IEEE*, 2010, vol. 98, no. 6, p. 1006–1020. DOI: 10.1109/JPROC.2009.2037526
- [10] PATEL, V. M., EASLEY, G. R., HEALY, D. M. Compressed synthetic aperture radar. *IEEE Journal of Selected Topics in Signal Processing*, 2010, vol. 4, no. 2, p. 244–254. DOI: 10.1109/JSTSP.2009.2039181
- [11] FENG, J., GONG, Z. ISAR imaging based on iterative reweighted Lp block sparse reconstruction algorithm. *Progress In Electromagnetics Research M*, 2016, vol. 48, p. 155–162. DOI: 10.2528/PIERM16041501
- [12] WEI, S., LIANG, J., WANG, M., et al. CIST: An improved isar imaging method using convolution neural network. *Remote Sensing*, 2020, vol. 12, no. 16, p. 2641. DOI: 10.3390/rs12162641

- [13] TROPP, J. A. Greed is good: Algorithmic results for sparse approximation. *IEEE Transactions on Information Theory*, 2004, vol. 50, no. 10, p. 2231–2242. DOI: 10.1109/TIT.2004.834793
- [14] NATARAJAN, B. K. Sparse approximate solutions to linear systems. *SIAM Journal on Computing*, 1995, vol. 24, no. 2, p. 227–234. DOI: 10.1137/S0097539792240406
- [15] DAUBECHIES, I., TESCHKE, G., VESE, L. A. Iteratively solving linear inverse problems under general convex constraints. *Inverse Problems and Imaging*, 2007, vol. 1, no. 1, p. 29–46. DOI: 10.3934/ipi.2007.1.29
- [16] DONOHO, D. L. For most large underdetermined systems of linear equations the minimal ℓ_1 -norm solution is also the sparsest solution. *Communications on Pure and Applied Mathematics*, 2006, vol. 59, no. 6, p. 797–829. DOI: 10.1002/cpa.20132
- [17] BOYD, S., VANDENBERGHE, L. *Convex Optimization*. Cambridge University Press, 2004. ISBN: 9780511804441, DOI: 10.1017/CBO9780511804441
- [18] CANDÉS, E. J., ROMBERG, J. K., TAO, T. Stable signal recovery from incomplete and inaccurate measurements. *Communications on Pure and Applied Mathematics*, 2006, vol. 59, no. 8, p. 1207–1223. DOI: 10.1002/cpa.20124
- [19] ZHANG, L., QIAO, Z. J., XING, M. D. High-resolution ISAR imaging by exploiting sparse apertures. *IEEE Transactions on Antennas and Propagation*, 2012, vol. 60, no. 2, p. 997–1008. DOI: 10.1109/TAP.2011.2173130
- [20] ZHANG, L., QIAO, Z. J., XING, M. D. High-resolution ISAR imaging with sparse stepped-frequency waveforms. *IEEE Transactions on Geoscience and Remote Sensing*, 2011, vol. 49, no. 11, p. 4630–4651. DOI: 10.1109/TGRS.2011.2151865
- [21] HASHEMPOUR, H. R. Sparsity-driven ISAR imaging based on two-dimensional ADMM. *IEEE Sensors Journal*, 2020, vol. 20, no. 22, p. 13349–13356. DOI: 10.1109/JSEN.2020.3006105
- [22] OZ, Y., ALP, Y. K., YAZGAN-ERER, I. ISAR imaging under group sparsity constraints using ADMM. In *Signal Processing and Communications Applications Conference (SIU)*. Gaziantep (Turkey), 2020, p. 1–4. DOI: 10.1109/SIU49456.2020.9302303
- [23] LI, S. D., CHEN, F. W., YANG, J., et al. A novel 2D complex FISTA for ISAR imaging. In *IET International Radar Conference*. Hangzhou (China), 2015, p. 1–4. DOI: 10.1049/cp.2015.0995
- [24] CANDÉS, E. J., WAKIN, M. B., BOYD, S. P. Enhancing sparsity by reweighted ℓ_1 minimization. *Journal of Fourier Analysis and Applications*, 2008, vol. 14, no. 5, p. 877–905. DOI: 10.1007/s00041-008-9045-x
- [25] CHARTRAND, R., STANEVA, V. Restricted isometry properties and nonconvex compressive sensing. *Inverse Problems*, 2008, vol. 24, no. 3, p. 1–14. DOI: 10.1088/0266-5611/24/3/035020
- [26] FOU CART, S., LAI, M. J. Sparsest solutions of underdetermined linear systems via ℓ_q -minimization for $0 < q \leq 1$. *Applied and Computational Harmonic Analysis*, 2009, vol. 26, no. 3, p. 395–407. DOI: 10.1016/j.acha.2008.09.001
- [27] SUN, Q. Recovery of sparsest signals via L_q -minimization. *Applied and Computational Harmonic Analysis*, 2012, vol. 32, no. 3, p. 329–341. DOI: 10.1016/j.acha.2011.07.001
- [28] WU, Y. M., WU, A. W., JIN, Y. Q., et al. An efficient method on ISAR image reconstruction via norm regularization. *IEEE Journal on Multiscale and Multiphysics Computational Techniques*, 2019, vol. 4, p. 290–297. DOI: 10.1109/JMMCT.2019.2953880
- [29] WU, A., WU, Y., JIN, Y., et al. $L(1/2)$ regularization for ISAR imaging and target enhancement of complex image. *IEEE Transactions on Geoscience and Remote Sensing*, 2020, vol. 60, p. 1–10. DOI: 10.1109/TGRS.2020.3040277
- [30] ZHANG, S., LIU, Y., LI, X., et al. Enhancing ISAR image efficiently via convolutional reweighted ℓ_1 minimization. *IEEE Transactions on Image Processing*, 2021, vol. 30, p. 4291–4304. DOI: 10.1109/TIP.2021.3070442
- [31] FIGUEIREDO, M. A. T., BIOCAS-DIAS, J. M., NOWAK, R. Majorization-minimization algorithms for wavelet-based image restoration. *IEEE Transactions on Image Processing*, 2007, vol. 16, no. 12, p. 2980–2991. DOI: 10.1109/TIP.2007.909318
- [32] ZHAO, Y., WU, C., DONG, Q., et al. An accelerated majorization-minimization algorithm with convergence guarantee for non-Lipschitz wavelet synthesis model. *Inverse Problems*, 2022, vol. 38, no. 1, p. 1–37. DOI: 10.1088/1361-6420/ac38b8
- [33] BECK, A., TEOULLE, M. A fast iterative shrinkage-thresholding algorithm for linear inverse problems. *SIAM Journal on Imaging Sciences*, 2009, vol. 2, no. 1, p. 183–202. DOI: 10.1137/080716542
- [34] WU, C., TAI, X. Augmented Lagrangian method, dual methods, and split Bregman iteration for ROF, vectorial TV, and high order models. *SIAM Journal on Imaging Sciences*, 2010, vol. 3, no. 3, p. 300–339. DOI: 10.1137/090767558

About the Authors . . .

Yanan ZHAO received the Ph.D. degree in Computational Mathematics from the Nankai University, in 2022. Currently, she works at the Nanjing Research Institute of Electronic Engineering, her research interests include non-convex optimization theory and sparse signal reconstruction.

Fengyuan YANG received the Ph.D. degree in Electrical Engineering from the Shanghai Jiaotong University, in 2018. Currently, he works at the Nanjing Research Institute of Electronic Engineering, his research interest is compressed sensing.

Chao WANG received the Ph.D. degree in Mechanical Engineering from the Nanjing University of Science and Technology, in 2017. Currently, he works at the Nanjing Research Institute of Electronic Engineering, his research interest is image processing.

Fangjie YE received the B.S degree in Computational Mathematics from the Nankai University, in 2019. His research interests include numerical calculation and machine learning.

Feng ZHU received the B.S degree in Computational Mathematics from the Jilin University, in 2002. Currently, he works at the Nanjing Research Institute of Electronic Engineering, his research interest is radar imaging.

Yu LIU received the M.S degree in Signal and Information Processing from the Harbin Engineering University, in 2011. Currently, he works at the Nanjing Research Institute of Electronic Engineering, his research interest is radar imaging.